

Bidirectional Sparse Attention for Faster Video Diffusion Training

Chenlu Zhan^{1*} Wen Li^{1*} Chuyu Shen¹ Jun Zhang¹ Suhui Wu¹ Hao Zhang^{1†}
¹ByteDance

zhanchenlu@bytedance.com, liwen.8459@bytedance.com, zhanghao.25@bytedance.com

Abstract

Video diffusion Transformer (DiT) models excel in generative quality but hit major computational bottlenecks when producing high-resolution, long-duration videos. The quadratic complexity of full attention ($O(L^2)$) leads to prohibitively high training and inference costs. Full attention inefficiency stems from two key challenges: excessive computation due to the inherent sparsity of Queries and Key-Value pairs, and redundant computation as fixed sparse patterns fail to leverage DiT’s dynamic attention. To overcome this limitation, we propose a Bidirectional Sparse Attention (BSA) framework for faster video DiT training, the first to dynamically sparsify both Queries and Key-Value pairs within 3D full attention, thereby substantially improving training and inference efficiency. BSA addresses these issues through two key components. Query sparsity is optimized by selecting the most informative query tokens via semantic similarity and with a dynamic spatial-time training strategy, while KV sparsity is achieved by computing a statistical dynamic threshold to retain only the most salient KV blocks for computation. Extensive experiments demonstrate that BSA significantly accelerates DiT training across long sequences, reducing FLOPs by up to $20\times$ and achieving $17.79\times$ faster attention training, while preserving or even surpassing the generative quality of full attention.

1. Introduction

Modeling long sequences remains a pivotal challenge in deep learning, particularly for video diffusion models (VDMs) designed to generate high-resolution, long-duration videos [17, 18, 22]. Although full attention is powerful, its quadratic complexity with respect to sequence length ($O(L^2)$) severely limits scalability. Even a brief few-second video clip can expand into hundreds of thousands of tokens, making attention computation the primary bottleneck in video Diffusion Transformers (DiTs) [12, 16, 23, 28]. Moreover, attention operations account for over 90%

*Equal Contribution.

†Project Leader. Corresponding Author.

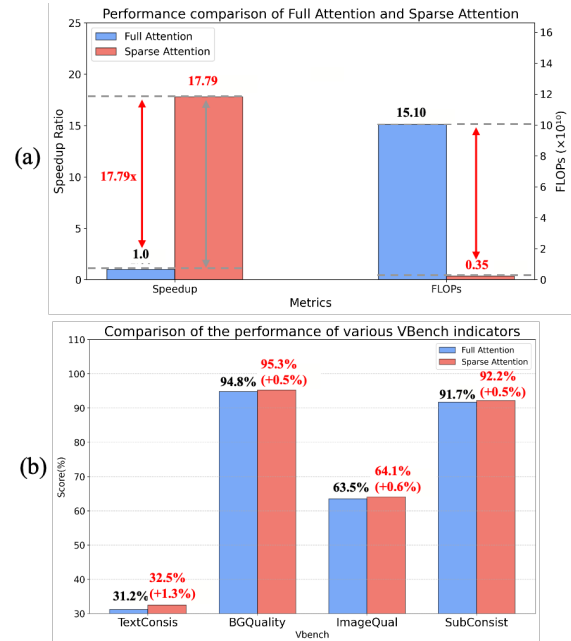


Figure 1. (a) Speedup ratio and computational cost comparison between Sparse Attention and Full Attention. (b) Comparison of generation quality across four consistency metrics on VBench [10].

of training costs in VDMs, highlighting the critical need for efficient and trainable sparse attention mechanisms.

To design an efficient trainable sparse attention mechanism, we first pinpoint two primary sources of training latency: **(1) Bilateral Redundancy**. As shown in Fig. 2, we utilize query-key similarity visualization to discern the semantic features of each query. The heatmap of full attention queries in Frames 3-12 reveals highly similar representations, suggesting that these query tokens are semantically redundant. Besides, only a small subset of KV pairs contributes meaningfully to each query [15, 29, 33]. It means that significant redundancy exists on both the Query and Key-Value sides. **(2) Dynamic Sparsity**. DiT attention is inherently dynamic [21]. Each query’s matching critical subset of KV pairs dynamically changes [24]. Besides,

the sparsity of different local KV subsets varies dynamically at different training times and between different local KV subsets [21]. Recent works [15, 21, 29, 33] indeed introduce sparse attention to accelerate training or inference. They achieve this by restricting each query to a fixed subset of KV pairs to reduce computation [15, 33]. However, fixed sparsity patterns are parameter-sensitive, and over or under sizing can cause redundancy and performance loss, failing to adapt to real dynamic sparsity. Moreover, most methods [25, 32] only prune KV pairs, ignoring query-side redundancies like repeated semantics across frames, which further inflate costs. Overall, these sparse methods have not fully adapted to the sparsity discoveries in attention, remaining limited.

To address the above challenges, we propose (**BSA**, a **Bidirectional Sparse Attention**), a novel framework designed to accelerate video diffusion training. Our primary contribution is the first explicit analysis that leverages the inherent sparsity in Query, combining it with KV sparsity to formulate a bidirectional sparse-attention mechanism. This approach is further enhanced by a dynamic adjustment strategy that achieves adaptive sparsity tuning. Specifically, our method differs in two major aspects: (1) **Dynamic Query Sparsity**. We begin by partitioning long-sequence tokens into 3D blocks. For query sparsity, we preserve tokens with distinctive information and prune redundant ones based on their similarity to the block’s center token. Furthermore, we incorporate a temporal dynamic sparsity strategy to adaptively capture global-to-local semantic variations during training. (2) **Dynamic Statistic KV Sparsity**. For KV-sparsity, we dynamically identify the most relevant KV tokens for each query. Using block-wise attention scores, we compute statistic thresholds and iteratively admit tokens until a cumulative score target is reached. Our approach is model-agnostic and can be applied to any DiT architecture. We implement BSA on Wan2.1-1.3B model with from-scratch training. Extensive experiments demonstrate that BSA significantly accelerates training, as shown in Fig. 1, achieving up to **20×** reduction in FLOPs and **17.79×** faster attention computation, while preserving or even surpassing the generative quality of full attention. Additionally, our model improves the efficiency of inference without compromising the quality of output, reducing end-to-end latency on an H100 GPU with a **6.2×** speedup. Our contributions are summarized as follows:

- We present BSA, a trainable bidirectional dynamic sparse-attention framework, which for the first time orthogonally sparsifies Query and Key–Value pairs within full attention to accelerate video diffusion training.
- We devise distinct dynamic sparsity strategies for Queries and KV blocks, effectively capturing attention variability during training and enabling adaptive token selection beyond fixed patterns.

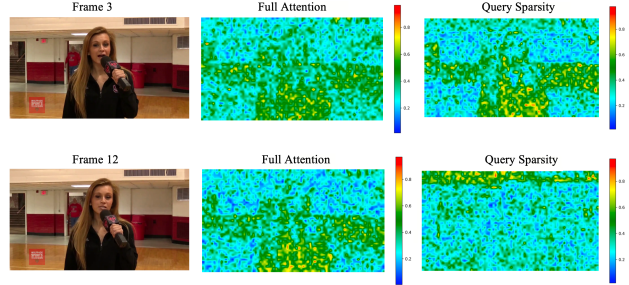


Figure 2. Redundancy in spatiotemporal representations of videos. We employ query-key similarity visualization to discern the semantic features of each query. The heatmap of full attention in Frames 3-12 reveals highly similar representations, indicating semantic redundancy among these query tokens. Post-query sparsification, attention visualization features in different frames exhibit distinct semantic representations. This underscores our query sparsification’s ability to eliminate redundant semantic features and select the most critical queries to preserve the original semantic representations.

- Extensive experiments on Wan2.1-1.3B demonstrate that BSA delivers up to 20× FLOPs reduction, 17.7× training speedups, and 6× inference acceleration, while maintaining or surpassing the generative quality of full attention.

2. Related Work

General Sparse Attention. Sparse attention has been widely adopted in Large Language Models (LLMs) [1, 3, 5–7, 13, 14] and Vision–Language Models (VLMs) [19] to mitigate the computational explosion caused by long input sequences. Most methods, however, fix sparsity a priori. For instance, LLM schemes [8, 26] exploit attention concentration on early or local tokens. SeerAttentions [5, 6] chiefly prune token redundancy under causal masks. MInference [11] leverages head-wise heterogeneous sparsity. However, these techniques are limited to predefined patterns, neglecting the inherent dynamic redundancy of video data and are typically optimized for inference acceleration rather than training. To tackle this, recent methods like MoBA [15] and NSA [29] explore trainable dynamic sparsity for end-to-end acceleration on long sequences. However, these works concentrate solely on redundancy in Key–Value pairs, disregarding dynamic redundancy in Queries. Besides, they frequently depend on fixed selection rules that fail to adapt to the inherently dynamic sparsity of sequences, leading to additional computational overhead.

Sparse Attention for Video Diffusion. Recent studies [2, 9, 14, 21, 25, 27, 31] have attempted to transfer sparse attention from LLMs to video DiTs, primarily for inference acceleration. However, training-free schemes are not suitable for video pre-training for two reasons. First, fixed sparsity patterns hinge on brittle hyperparameters [15, 33].

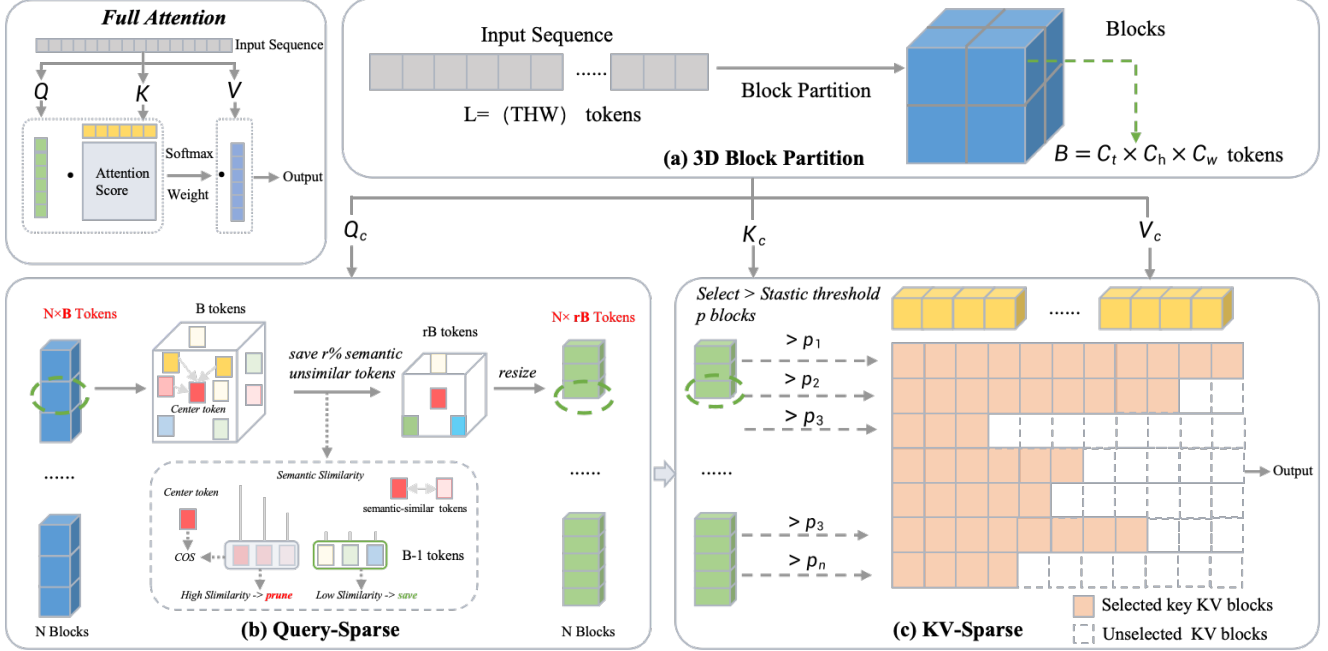


Figure 3. Overview of BSA. We introduce a Bidirectional Attention Sparsification that exploits the dynamic sparsity of both Queries and Key-Value (KV) pairs. (a) We first partition the video sequence into blocks to efficiently select critical tokens (Sec. 3.2.1). (b) We then select each block’s center token, linearly score within-block tokens by semantic similarity to the center, and prune a fixed fraction of redundant tokens to retain only the most informative queries (Sec. 3.2.2). (c) For KV sparsity, we dynamically pick the most relevant KV tokens per query. We compute sparsity-adaptive thresholds and iteratively admit tokens until a cumulative score target is met (Sec. 3.2.3).

With far longer video sequences, such static patterns often erode generative quality and induce artifacts [25, 31]. Second, the chief bottleneck in video DiTs is quadratic attention over long sequences, impacting both training and inference. Hence, boosting training efficiency requires a trainable sparse-attention mechanism. While VSA [33] and VMoBA [24] offer partial relief, they remain suboptimal. VSA [33] is bound by fixed block sizes and top-k selection, whereas VMoBA [24] swaps top-k for thresholding yet remains highly sensitive to threshold and block design. Moreover, both methods overlook query-side redundancy that cannot track the intrinsic dynamics of video sequences, leading to wasteful computation. To address this, we propose a bidirectional sparse-attention scheme that dynamically prunes both Queries and Key-Value pairs, eliminating redundant features while maintaining generative fidelity.

3. Method

In this section, we introduce the **BSA**, a **B**idirectional **A**ttention **S**parsification method that exploits the dynamic sparsity of both Queries and Key-Value (KV) pairs. Our method removes query-side redundancy and adaptively selects salient KV pairs, yielding near-optimal bidirectional optimization under quadratic attention. Specifically, Sec. 3.1 surveys the key components and motivation of

sparse attention; Sec. 3.2.1 presents KV block partitioning, and Sec. 3.2.2 details the query-side dynamic sparsification. We describe the dynamic statistic KV-sparse in Sec. 3.2.3. We also introduce the specific kernel design in Sec. 3.3.

3.1. Review of Sparse Attention

Modern video DiTs use 3D full attention to model dependencies across the entire spatiotemporal volume. Given a latent tensor (T, H, W) , each token at (t, h, w) is flattened to a 1D index $n = tHW + hW + w$, yielding a sequence of length $L = THW$. Full attention is then applied to this sequence, enabling all-to-all token interactions. For a single attention head, let $Q, K, V \in \mathbb{R}^{L \times d}$ denote the query, key, and value matrices, and let $M \in \{-\infty, 0\}^{L \times L}$ denote the attention mask that specifies the allowed token-to-token connections. The attention output O is computed as:

$$S = \frac{QK_s^\top}{\sqrt{d_k}}, \quad O = \text{Softmax}(S)V_s. \quad (1)$$

In full attention, all sequence tokens from $Q, K,$ and V participate in interaction and computation. Sparse attention, which theoretically reduces overall computation by selecting a key subset K_s and V_s from the KV pairs, aims to improve efficiency. However, since modern accelerators are heavily optimized for dense computation, unstructured sparsity remains difficult to convert into a practical speedup.

3.2. BSA Structure

As illustrated in Fig.3, our framework consists of three main components: (a) **3D Block Partition**. The video latent is divided into spatiotemporal blocks via average pooling to efficiently filter critical information. (b) **Query-Sparse**. We efficiently select the most informative query tokens based on the redundancy within Queries, and design dynamic sparsity strategies that exploit spatiotemporal sparsity patterns. (c) **KV-Sparse**. For each query, we dynamically admit the most relevant KV tokens, iteratively accruing candidates until the cumulative score meets a target threshold. This removes predefined sparsity patterns and adapts to content-dependent variability.

3.2.1. Block Partition

Block-level Query Representation. Given a video of shape (T, H, W) , to efficiently select a subset of critical tokens with reduced computational cost, we first group multiple tokens into blocks. For input queries Q , keys K , and values V , the video latent (T, H, W) is partitioned into blocks of size (C_t, C_h, C_w) , where each block corresponds to a GPU block, and the block size is $B = C_t \times C_h \times C_w$. Tokens within each block are average-pooled to obtain block-level queries Q_c , keys K_c , and values V_c .

3D-to-1D Indexing. We assume that the video latent dimensions (T, H, W) are divisible by the block sizes, and define $(N_t, N_h, N_w) = (T/C_t, H/C_h, W/C_w)$. When flattening the 3D video into a 1D sequence, each token at position (t, h, w) is assigned a 1D index n . Leveraging block partitioning, we can efficiently localize critical tokens without materializing the full attention matrix A . Yet attention remains token-level and computationally dominant. Thus, our core objective is to select effective tokens for computation while eschewing redundant work.

3.2.2. Query-Sparse

Video data intrinsically contains temporal dependencies across frames and spatial coherence within frames, leading to substantial spatiotemporal redundancy. Empirical results show that just 4% of spatially adjacent tokens contribute to 80% of attention scores in video diffusion models, indicating most tokens are redundant [20]. Noting that core semantics depend on a few key query tokens. However, Query sparsification is challenging because it alters sequence length. Removing redundant tokens while preserving semantic meaning and maintaining the original length is nontrivial. We address this by propose a feature-redundancy-based query-sparse method to eliminate redundancy, reshaping the sparse queries into smaller blocks for efficient attention computation, and reindexing outputs to restore the original sequence length. Given a query sequence Q partitioned into N blocks Q_c , let $Q_c^{(b)}$ denote the tokens in block b and $q_c^{(b)}$ its center token. Tokens within

a block (e.g., spatial neighbors) typically share similar features, allowing $q_c^{(b)}$ to represent the block. We thus measure the cosine similarity between each token and $q_c^{(b)}$, preserving local distinctions and avoiding the uniformity of average pooling.

For each block, token similarity is evaluated linearly, and only non-redundant tokens are retained. These selected tokens drive key attention scores, while redundant ones, whose features are largely duplicative, are safely pruned without loss of performance or semantic integrity. For each block, a pruning ratio r is applied to retain a portion of tokens, and the retained tokens from all blocks are concatenated to form a new redundancy-free query Q^s , defined as:

$$Q^s = \bigcup_{b=1}^N \left\{ q_i \in Q_c^{(b)} \mid \text{rank}_b(1 - \cos(q_c^{(b)}, q_i)) \leq \lceil r \cdot |Q_c^{(b)}| \rceil \right\} \quad (2)$$

where $\text{rank}_b(\cdot)$ is the ranking within block in descending order, N is the number of blocks. $|Q_c^{(b)}|$ is the number of tokens in block b , and $r \in (0, 1]$ is the retention ratio.

To enhance critical token selection, we adopt a window-based mechanism: each block query is further partitioned into smaller windows of size (w_t, w_h, w_w) , evenly dividing the block (C_t, C_h, C_w) . Within each window, the center token is chosen and its similarity to neighboring tokens is computed via cosine similarity or dot product. Tokens selected from all windows are then concatenated, effectively preserving non-redundant, semantically important tokens.

3.2.3. KV-Sparse

Building on block-level representations from cuboid partitioning, each query interacts with only a subset of KV pairs, greatly reducing computational cost. However, optimally selecting these KV subsets per query remains challenging. Our experiments show that sparsity varies significantly both across and within attention blocks, and the relevant KV pairs for each query are highly dynamic. Thus, a fixed strategy fails to adaptively assign KV pairs. Over-selection leads to computational redundancy, whereas under-selection results in accuracy loss. To address this, we propose a *dynamic KV-Sparse* method based on statistical thresholds, which adaptively selects the relevant KV pairs for each query. The sparsity threshold is determined from the input attention scores, eliminating the need for pre-defined sparse patterns and enabling adaptation to diverse input content. Our dynamic sparsity manifests in two aspects:

Computation of statistical dynamic threshold. Specifically, given inter-block attention scores s_b for a computation, we aim to select k key KV pairs. Since the distribution of s_b varies across inputs, a fixed k may fail to capture truly critical KV pairs. We therefore compute a dynamic threshold p based on the mean and standard deviation of the attention scores, such that k key samples are selected:

$$p = \text{mean}(S_b) + \text{std}(S_b) \cdot U(1 - k/n), \quad (3)$$

where n is the number of inter-block attention scores, $1 \leq k \leq n$ is the number of desired key samples, and $U(\cdot)$ denotes the quantile function.

Dynamic selection of key KV pairs per query. For the selected key blocks (assume K in total), each query block computes attention with the KV pairs and dynamically selects indices. For query block i , the minimal index set S_i is chosen such that the cumulative attention satisfies:

$$\gamma(\min |S_i| \text{ s.t. } \sum_{(i,j) \in S_i} \frac{\exp(Q_i K_j^\top)}{\sum_{j'} \exp(Q_i K_{j'}^\top)} \geq p) \quad (4)$$

while γ denotes the operation that returns the minimal index set S_i . The results from all query blocks are then aggregated.

3.2.4. Computation Cost Analysis

Let the sparsified query matrix be $Q^s \in \mathbb{R}^{rL \times d}$, where rL is the number of sparsified query tokens, and the selected key and value matrices are K_S and V_S , defined as $K_S = \{K_j \mid j \in \bigcup_i S_i\}$, $V_S = \{V_j \mid j \in \bigcup_i S_i\}$. The sparse mask M_S ensures attention is computed only between selected queries and KV pairs. The sparse attention output O^s is expressed as:

$$S^s = \frac{Q^s K_S^\top}{\sqrt{d_k}}, \quad O^s = \text{Softmax}(S^s) V_S \quad (5)$$

where $S^s \in \mathbb{R}^{rL \times L_S}$ is the sparsification attention score matrix (L_S is the number of selected KV tokens), A^s is the normalized sparse attention weight matrix, $\sqrt{d_k}$ is the scaling factor, and O^s has the same sequence length as the input. We also provide a detailed analysis of the additional computational overhead introduced by our proposed query-sparse and KV-sparse methods. For query-sparse, we compute intra-block token similarity and perform sorting over the sequence, resulting in a total computational complexity of $O(L) + O(L \log L)$, where L is the sequence length. For KV-sparse, similarity computation and sorting are performed between each query block and KV block, with a total complexity of $O(N) + O(N)$, where N is the number of blocks. It is important to emphasize that the additional computation introduced by query and KV sparsification accounts for less than 0.1% of the total FLOPs, making it a negligible cost.

3.3. Kernel Design

We implement separate forward and backward kernels with Triton, enabling hardware-efficient block-sparse attention for Flash Attention-level acceleration in training and pre-filling. By partitioning the attention mask into blocks, each GPU SM tile can process or skip blocks entirely, maximizing hardware efficiency where dense computation is preferred.

Query-sparse design creates block-level sparsity with variable block sizes. We use tailored kernels and mapping

indices to compute only relevant pairs, maintaining dimension consistency. In both forward and backward passes, sparsity masks and mappings align blocks and filter excess tokens, ensuring proper computation throughout.

Our KV-sparse strategy adaptively selects variable-sized key KV pairs for each query, using custom kernels for efficient computation. Each Q block records its attended KV blocks with $q2k_num$ and $q2k_index$, enabling distinct selections. Attention weights are computed and aggregated block-wise, with all outputs concatenated to form the final attention result. More details are in the supplemental.

4. Experiment

4.1. Dataset and Implement

Datasets. To train the baseline model and BSA from scratch, we selected 300k videos from the Vchitect [4] T2V DataVerse and conducted a three-step preprocessing pipeline: (1) **shot segmentation**, splitting multi-scene videos into single-scene clips; (2) **temporal truncation**, extracting 5-second clips from the segmented videos; (3) **caption generation**, employing the Tarsier2 [30] video description model to produce corresponding captions for each processed clip. The resulting 300k samples were further processed into different resolutions (448×832 and 782×1280) for ablation training, mitigating potential interference caused by varying resolutions and sequence lengths. In each experimental setting, all models were trained on the same dataset, and all configurations were kept consistent.

Metrics. We evaluate the generative capability of the models from training efficiency and generation quality. For training efficiency, we measure the acceleration ratio and computation FLOPs. For generative quality, we adopt the five evaluation dimensions of VBench [10], specifically: Text Consistency for overall coherence, Dynamic Degree for motion fidelity, BG Consistency for background consistency, Image Quality for visual fidelity, and Sub Consistency for subject-level consistency.

Baselines. In all experiments involving training models from scratch, we compare our sparse attention mechanism against full attention. Since our sparse attention is learnable, we additionally benchmark it against other sparse attention methods [24, 33] trained under the same objective.

Implement Details. We employ Wan2.1-1.3B [23] as the backbone model for all experiments. For block partitioning, we set B to a size of $(4, 4, 4)$ with 64 units per dimension. For Query-sparse pruning, the sparsity ratio r is set to 0.5, corresponding to a query block size of 32, and the window size is configured as $(2, 2, 2)$. Following prior baseline work, we adopt an annealed attention sparsity schedule: training begins with full attention, and every 30 steps, the sparsity is increased by 0.03 until reaching a maximum of 0.9. In KV-sparse, the number of top- k tokens selected is

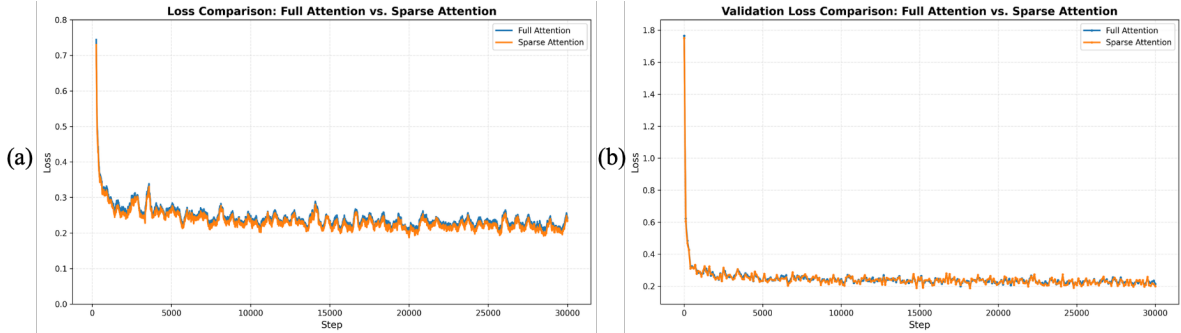


Figure 4. Comparison curves of (a) training loss and (b) validation loss for *Sparse Attention* and *Full Attention*.

Seq_len	Method	Sparsity	Quality				Efficiency	
			TextConsis \uparrow	BGConsis \uparrow	ImageQual \uparrow	SubConsist \uparrow	\downarrow FLOPs	SpeedUp \uparrow
61*448*832	Full Attention	-	32.71%	95.12%	64.33%	92.34%	1.51×10^{12}	-
23,296 tokens	Sparse Attention (Ours)	0.93	32.79%	95.22%	64.29%	92.39%	1.05×10^{11}	12.85x
157*768*1280	Full Attention	-	34.76%	93.26%	65.91%	93.79%	6.99×10^{13}	-
153,600 tokens	Sparse Attention (Ours)	0.95	34.93%	93.41%	66.03%	94.13%	3.49×10^{12}	17.79x

Table 1. The comparison of generation quality and efficiency between BSA and full attention, based on the Wan2.1-1.3B model.

gradually reduced from the total number of blocks to $0.1 \times$ the total, and the dynamic threshold is computed based on the varying k . Full training is conducted for 30,000 steps. All experiments are performed on NVIDIA H100 GPUs. Additional implementation details are provided in the Appendix.

4.2. Quantitative Results

4.2.1. Training-based Comparison

We perform all Text-to-video model training based on the Wan2.1-1.3B backbone, training all models to full convergence to ensure fair comparisons.

Loss Comparison. As shown in Fig. 4, both our proposed Sparse Attention and the Full Attention baseline exhibit stable and smooth pre-training loss curves. Notably, the loss curve of our Sparse Attention model consistently overlaps with that of the Full Attention model, and in most cases, it outperforms Full Attention. Figures 4 (a) and 5(b) illustrate the training and validation loss comparisons, respectively.

Efficiency and Quality Comparison. As summarized in Table 1, we conduct full scratch training of Sparse Attention and Full Attention on the Wan2.1-1.3B model at two different resolutions: the original resolution ($61 \times 448 \times 832$, 23K tokens) and an extended resolution with longer token sequences ($157 \times 768 \times 1280$, 153K tokens).

- **23K tokens:** Our Sparse Attention achieves a $12.85 \times$ speedup over Full Attention, attaining 93% sparsity and 7% of Full Attention FLOPs. BSA not only accelerates training but also surpasses Full Attention in generative quality on four VBench metrics, especially background consistency, showing it delivers faster training and better generation even on shorter sequences.

- **153K tokens:** The advantages of Sparse Attention become even more pronounced at longer sequence lengths. Compared to Full Attention, Sparse Attention achieves a $17.79 \times$ speedup, 95% sparsity, and 5% of Full Attention FLOPs. It achieves greater gains in text and background consistency, mainly because longer sequences allow higher sparsity and more acceleration.

Training on Longer Sequences. To assess BSA’s training speedup across different sequence lengths, we tested five lengths (23K, 44K, 59K, 117K, 153K tokens) with consistent settings. As shown in Fig. 6, speedup increases with sequence length, from $12.85 \times$ at 23K to $17.79 \times$ at 153K. These results demonstrate that our proposed Sparse Attention becomes increasingly effective at reducing training time as sequence length grows.

Sparse Adaptation. To explore how sparsity affects training loss and computational cost, we measured validation loss and FLOPs at various sparsity levels, as shown in Fig. 7. A sparsity of 0 represents Full Attention training. Sparsity in our model is controlled by the retained token ratio r for Query-sparse and the dynamic threshold p for KV-sparse, which selects top- k key tokens per attention scores. This creates a trade-off between efficiency and accuracy.

Fig. 7 shows that as sparsity increases from 0 to 0.93, validation loss remains stable near 0.212, matching Full Attention, while FLOPs drop. Beyond 0.95 sparsity, FLOPs keep decreasing, but validation loss rises sharply, indicating generation quality suffers. The best results are at 0.93 sparsity, where nearly lossless or better generation is achieved with a $13 \times$ FLOPs reduction. Notably, optimal sparsity depends on sequence length, longer sequences may benefit from higher sparsity. Our sparsity computation is more flex-



Figure 5. Qualitative comparison of text-to-video generation results between full attention and BSA across 4 different sequence lengths.

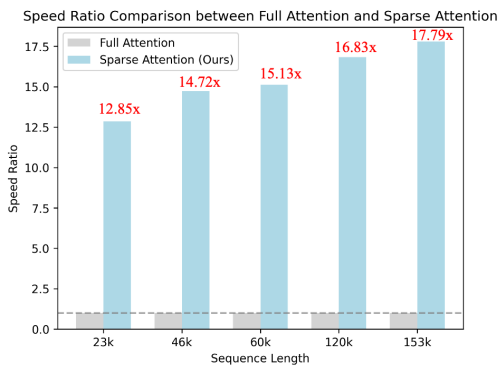


Figure 6. Speedup ratio of the attention under varying sequence lengths.

ible than fixed top-k methods, which require manual tuning for different sequence lengths and model sizes. Instead, our dynamic threshold automatically selects optimal keys based on the data, showing that effective sparse attention should adapt to the input rather than follow a fixed structure.

4.3. Qualitative Results.

As shown in Fig. 5, we compare video frames generated by Full Attention and our proposed Sparse Attention across different sequence lengths and resolutions.

As illustrated in Fig. 5, we present qualitative comparisons of T2V generation results across four representative cases, spanning different sequence lengths and resolutions (448×832 and 782×1280). For fairness, we sample the same frames from videos generated by Full Attention and our proposed Sparse Attention, selecting three representative frames for side-by-side comparison. Across all exam-

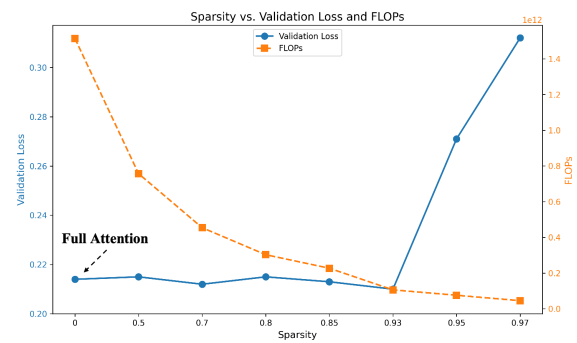


Figure 7. Validation loss and FLOPs under different sparsity levels..

ples, our BSA achieves generation quality comparable to Full Attention without perceptible degradation. As shown in Fig. 5, Sparse Attention consistently generates high-quality videos across various scenarios. It produces realistic facial expressions and movements (a), preserves fine details and precise alignment in complex scenes (b), faithfully renders textures in high-res landscapes (c), and maintains fidelity in challenging cases with intricate backgrounds and fur textures (d). More comparisons and generated videos are included in the supplementary material.

4.4. Comparison with Training-based Attentions

As shown in the Table 3, we provide a detailed comparison with the most relevant training-based sparse attention methods, such as MoBA [15] and VSA [33]. Our BSA achieves a clear advantage in speedup over both MoBA and VSA, and also delivers superior generation quality compared to these sparse attention approaches.

Method	Settings	Sparsity	Validation Loss	Quality				Efficiency	
				TextConsis \uparrow	BGConsis \uparrow	ImageQual \uparrow	SubConsist \uparrow	\downarrow FLOPs	SpeedUp \uparrow
Query-sparse	Original	0.5	0.211	32.83%	95.25%	64.34%	92.44%	7.5×10^{11}	1.96x
	w/ Window	0.5	0.208	32.85%	95.29%	64.36%	92.44%	7.5×10^{11}	1.98x
KV-sparse	Original	0.86	0.210	32.84%	95.24%	64.30%	92.41%	2.1×10^{11}	6.05x
	w/ Statistic	0.89	0.209	32.82%	95.25%	64.28%	92.42%	1.67×10^{11}	6.12x
Full Attention	-	0	0.213	32.71%	95.12%	64.33%	92.34%	1.51×10^{12}	-
Query-sparse+KV-sparse	-	0.93	0.212	32.79%	95.22%	64.29%	92.39%	1.73×10^{11}	12.85x

Table 2. Ablation Study. All ablation experiments are conducted at a sequence length of 23k to ensure fair comparison. Original (1st row): the selection of a key token in the whole query block rather than in a smaller window block. Window: window-based mechanism in query-sparse. Original (3rd row): the fixed threshold in kv-sparse. Statistic: statistical dynamic threshold in kv-sparse.

Seq_len	Method	Sparsity	Quality				Efficiency	
			TextConsis \uparrow	BGConsis \uparrow	ImageQual \uparrow	SubConsist \uparrow	\downarrow FLOPs	SpeedUp \uparrow
61*448*832 23,296 tokens	MoBA [15]	0.80	32.56%	95.14%	64.14%	92.05%	3.02×10^{11}	1.2x
	VSA [33]	0.87	32.65%	95.03%	64.25%	92.21%	1.96×10^{11}	4.5x
	Sparse Attention (Ours)	0.93	32.79%	95.22%	64.29%	92.39%	1.05×10^{11}	12.85x
157*768*1280 153,600 tokens	MoBA [15]	0.80	34.34%	93.05%	65.34%	93.49%	2.62×10^{12}	2.3x
	VSA [33]	0.87	34.72%	93.22%	65.87%	93.72%	4.54×10^{11}	6.2x
	Sparse Attention (Ours)	0.95	34.93%	93.41%	66.03%	94.13%	3.49×10^{12}	17.79x

Table 3. The comparison of generation quality and efficiency between BSA and the most related works, MoBA [15] and VSA [33].

4.5. Ablation Study

To investigate the impact of Query-sparse and KV-sparse on acceleration and generation quality, we conduct comprehensive ablation experiments, as shown in Table 2.

4.5.1. Query-Sparse

Original Query-Sparse. Without KV-sparsity, we first evaluate a baseline Query-sparse strategy. Each block selects a center token and prunes redundant tokens based on feature similarity. As shown in Row 1 of Table 2, with a prune rate $r=0.5$, validation loss is even lower than full attention, indicating lossless training. This achieves 50% sparsity and 1.96 \times speedup, halving computation. Query-sparse also consistently surpasses full attention on all VBench metrics, showing it removes redundant tokens while preserving meaningful queries.

Query-Sparse with Window Size Selection. We further extend Query-sparse by adopting multiple center tokens via window partitioning. Specifically, for a block of size (4, 4, 4), we split it into (2, 2, 2) windows, yielding 8 sub-blocks. A center token is selected within each window, and pruning is conducted locally. As shown in Row 2 of Table 2, this approach achieves lower validation loss and better VBench performance at the same sparsity and FLOPs, confirming that window-based selection more effectively preserves meaningful tokens and reduces redundancy.

4.5.2. KV-Sparse

Original KV-Sparse. Independent of Query-sparse, we test KV-sparsity with a fixed threshold p . As shown in Row 3, this method achieves 0.86 sparsity, a 6.05 \times acceleration, and an 8.6 \times reduction in FLOPs, while maintaining a validation loss comparable to that of full attention. Although a

slight drop is observed in the *ImageQual* metric, improvements in text, background, and subject consistency compensate, resulting in near-lossless generation quality overall.

KV-Sparse with Statistical Dynamic Threshold. We further enhance KV-sparsity by replacing the fixed p with a dynamic threshold, adaptively computed from the attention score distribution within each block. As shown in Row 4 of Table 2, this approach achieves higher sparsity and greater acceleration with similar validation loss. It enables KV-sparsity to adjust to block redundancy, overcoming fixed k limitations. By using input-dependent attention scores, it selects more informative KV pairs, resulting in lower validation loss and better generative quality.

Query-Sparse + KV-Sparse. Combining Query-sparse and KV-sparse (Row 6, Table 2) achieves the best results: 0.93 sparsity and a 12.85 \times speedup, with validation loss and generation quality matching or exceeding those of full attention. Their orthogonality allows additive sparsity gains without sacrificing quality, confirming the effectiveness of our design. Additionally, the extra computational overhead is negligible, highlighting the practical efficiency of our sparsification strategies.

5. Conclusion

In this work, we presented BSA, a trainable sparse attention framework that jointly sparsifies Queries and Key-Value pairs within 3D full attention. By exploiting the inherent and dynamic sparsity of video sequences, BSA achieves substantial reductions in FLOPS and training time while maintaining, or even surpassing, the generative quality of full attention. Extensive experiments validate that BSA scales efficiently to video diffusion models, offering a practical solution to the computational bottlenecks of DiTs.

References

- [1] Iz Beltagy, Matthew E Peters, and Arman Cohan. Longformer: The long-document transformer. *arXiv preprint arXiv:2004.05150*, 2020. 2
- [2] Hangliang Ding, Dacheng Li, Runlong Su, Peiyuan Zhang, Zhijie Deng, Ion Stoica, and Hao Zhang. Efficient-vdit: Efficient video diffusion transformers with attention tile. *arXiv preprint arXiv:2502.06155*, 2025. 2
- [3] Jiayu Ding, Shuming Ma, Li Dong, Xingxing Zhang, Shao-han Huang, Wenhui Wang, Nanning Zheng, and Furu Wei. Longnet: Scaling transformers to 1,000,000,000 tokens. *arXiv preprint arXiv:2307.02486*, 2023. 2
- [4] Weichen Fan, Chenyang Si, Junhao Song, Zhenyu Yang, Yanan He, Long Zhuo, Ziqi Huang, Ziyue Dong, Jingwen He, Dongwei Pan, et al. Vchitect-2.0: Parallel transformer for scaling up video diffusion models. *arXiv preprint arXiv:2501.08453*, 2025. 5
- [5] Yizhao Gao, Zhichen Zeng, Dayou Du, Shijie Cao, Peiyuan Zhou, Jiaying Qi, Junjie Lai, Hayden Kwok-Hay So, Ting Cao, Fan Yang, et al. Seerattention: Learning intrinsic sparse attention in your llms. *arXiv preprint arXiv:2410.13276*, 2024. 2
- [6] Yizhao Gao, Shuming Guo, Shijie Cao, Yuqing Xia, Yu Cheng, Lei Wang, Lingxiao Ma, Yutao Sun, Tianzhu Ye, Li Dong, et al. Seerattention-r: Sparse attention adaptation for long reasoning. *arXiv preprint arXiv:2506.08889*, 2025. 2
- [7] Mandy Guo, Joshua Ainslie, David Uthus, Santiago Ontanon, Jianmo Ni, Yun-Hsuan Sung, and Yinfei Yang. Longt5: Efficient text-to-text transformer for long sequences. *arXiv preprint arXiv:2112.07916*, 2021. 2
- [8] Chi Han, Qifan Wang, Wenhan Xiong, Yu Chen, Heng Ji, and Sinong Wang. Lm-infinite: Simple on-the-fly length generalization for large language models. 2023. 2
- [9] Ali Hassani, Fengzhe Zhou, Aditya Kane, Jiannan Huang, Chieh-Yun Chen, Min Shi, Steven Walton, Markus Hoehnerbach, Vijay Thakkar, Michael Isaev, et al. Generalized neighborhood attention: Multi-dimensional sparse attention at the speed of light. *arXiv preprint arXiv:2504.16922*, 2025. 2
- [10] Ziqi Huang, Yanan He, Jiashuo Yu, Fan Zhang, Chenyang Si, Yuming Jiang, Yuanhan Zhang, Tianxing Wu, Qingyang Jin, Nattapol Chanpaisit, et al. Vbench: Comprehensive benchmark suite for video generative models. In *Proceedings of the IEEE/CVF Conference on Computer Vision and Pattern Recognition*, pages 21807–21818, 2024. 1, 5
- [11] Huiqiang Jiang, Yucheng Li, Chengruidong Zhang, Qianhui Wu, Xufang Luo, Surin Ahn, Zhenhua Han, Amir H Abdi, Dongsheng Li, Chin-Yew Lin, et al. Minference 1.0: Accelerating pre-filling for long-context llms via dynamic sparse attention. *Advances in Neural Information Processing Systems*, 37:52481–52515, 2024. 2
- [12] Weijie Kong, Qi Tian, Zijian Zhang, Rox Min, Zuozhuo Dai, Jin Zhou, Jiangfeng Xiong, Xin Li, Bo Wu, Jianwei Zhang, et al. Hunyuanvideo: A systematic framework for large video generative models. *arXiv preprint arXiv:2412.03603*, 2024. 1
- [13] Xunhao Lai, Jianqiao Lu, Yao Luo, Yiyuan Ma, and Xun Zhou. Flexprefill: A context-aware sparse attention mechanism for efficient long-sequence inference. *arXiv preprint arXiv:2502.20766*, 2025. 2
- [14] Chao Lou, Zixia Jia, Zilong Zheng, and Kewei Tu. Sparser is faster and less is more: Efficient sparse attention for long-range transformers. *arXiv preprint arXiv:2406.16747*, 2024. 2
- [15] Enzhe Lu, Zhejun Jiang, Jingyuan Liu, Yulun Du, Tao Jiang, Chao Hong, Shaowei Liu, Weiran He, Enming Yuan, Yuzhi Wang, et al. Moba: Mixture of block attention for long-context llms. *arXiv preprint arXiv:2502.13189*, 2025. 1, 2, 7, 8
- [16] Guoqing Ma, Haoyang Huang, Kun Yan, Liangyu Chen, Nan Duan, Shengming Yin, Changyi Wan, Ranchen Ming, Xiaoniu Song, Xing Chen, et al. Step-video-t2v technical report: The practice, challenges, and future of video foundation model. *arXiv preprint arXiv:2502.10248*, 2025. 1
- [17] William Peebles and Saining Xie. Scalable diffusion models with transformers. In *Proceedings of the IEEE/CVF international conference on computer vision*, pages 4195–4205, 2023. 1
- [18] Robin Rombach, Andreas Blattmann, Dominik Lorenz, Patrick Esser, and Björn Ommer. High-resolution image synthesis with latent diffusion models. In *Proceedings of the IEEE/CVF conference on computer vision and pattern recognition*, pages 10684–10695, 2022. 1
- [19] Leqi Shen, Guoqiang Gong, Tao He, Yifeng Zhang, Pengzhang Liu, Sicheng Zhao, and Guiguang Ding. Fastvid: Dynamic density pruning for fast video large language models. *arXiv preprint arXiv:2503.11187*, 2025. 2
- [20] Wenhao Sun, Rong-Cheng Tu, Yifu Ding, Zhao Jin, Jingyi Liao, Shunyu Liu, and Dacheng Tao. Vorta: Efficient video diffusion via routing sparse attention. *arXiv preprint arXiv:2505.18809*, 2025. 4
- [21] Xin Tan, Yuetao Chen, Yimin Jiang, Xing Chen, Kun Yan, Nan Duan, Yibo Zhu, Daxin Jiang, and Hong Xu. Dsv: Exploiting dynamic sparsity to accelerate large-scale video dit training. *arXiv preprint arXiv:2502.07590*, 2025. 1, 2
- [22] Ashish Vaswani, Noam Shazeer, Niki Parmar, Jakob Uszkoreit, Llion Jones, Aidan N Gomez, Łukasz Kaiser, and Illia Polosukhin. Attention is all you need. *Advances in neural information processing systems*, 30, 2017. 1
- [23] Team Wan, Ang Wang, Baole Ai, Bin Wen, Chaojie Mao, Chen-Wei Xie, Di Chen, Feiwu Yu, Haiming Zhao, Jianxiao Yang, et al. Wan: Open and advanced large-scale video generative models. *arXiv preprint arXiv:2503.20314*, 2025. 1, 5
- [24] Jianzong Wu, Liang Hou, Haotian Yang, Xin Tao, Ye Tian, Pengfei Wan, Di Zhang, and Yunhai Tong. Vmoba: Mixture-of-block attention for video diffusion models. *arXiv preprint arXiv:2506.23858*, 2025. 1, 3, 5
- [25] Haocheng Xi, Shuo Yang, Yilong Zhao, Chenfeng Xu, Muyang Li, Xiuyu Li, Yujun Lin, Han Cai, Jintao Zhang, Dacheng Li, et al. Sparse videogen: Accelerating video diffusion transformers with spatial-temporal sparsity. *arXiv preprint arXiv:2502.01776*, 2025. 2, 3
- [26] Guangxuan Xiao, Yuandong Tian, Beidi Chen, Song Han, and Mike Lewis. Efficient streaming language models with attention sinks. *arXiv preprint arXiv:2309.17453*, 2023. 2

- [27] Shuo Yang, Haocheng Xi, Yilong Zhao, Muyang Li, Jintao Zhang, Han Cai, Yujun Lin, Xiuyu Li, Chenfeng Xu, Kelly Peng, et al. Sparse videogen2: Accelerate video generation with sparse attention via semantic-aware permutation. *arXiv preprint arXiv:2505.18875*, 2025. [2](#)
- [28] Zhuoyi Yang, Jiayan Teng, Wendi Zheng, Ming Ding, Shiyu Huang, Jiazheng Xu, Yuanming Yang, Wenyi Hong, Xiaohan Zhang, Guanyu Feng, et al. Cogvideox: Text-to-video diffusion models with an expert transformer. *arXiv preprint arXiv:2408.06072*, 2024. [1](#)
- [29] Jingyang Yuan, Huazuo Gao, Damai Dai, Junyu Luo, Liang Zhao, Zhengyan Zhang, Zhenda Xie, YX Wei, Lean Wang, Zhiping Xiao, et al. Native sparse attention: Hardware-aligned and natively trainable sparse attention. *arXiv preprint arXiv:2502.11089*, 2025. [1](#), [2](#)
- [30] Liping Yuan, Jiawei Wang, Haomiao Sun, Yuchen Zhang, and Yuan Lin. Tarsier2: Advancing large vision-language models from detailed video description to comprehensive video understanding. *arXiv preprint arXiv:2501.07888*, 2025. [5](#)
- [31] Zhihang Yuan, Hanling Zhang, Lu Pu, Xuefei Ning, Linfeng Zhang, Tianchen Zhao, Shengen Yan, Guohao Dai, and Yu Wang. Ditfastattn: Attention compression for diffusion transformer models. *Advances in Neural Information Processing Systems*, 37:1196–1219, 2024. [2](#), [3](#)
- [32] Jintao Zhang, Chendong Xiang, Haofeng Huang, Jia Wei, Haocheng Xi, Jun Zhu, and Jianfei Chen. Spargeattn: Accurate sparse attention accelerating any model inference. *arXiv preprint arXiv:2502.18137*, 2025. [2](#)
- [33] Peiyuan Zhang, Haofeng Huang, Yongqi Chen, Will Lin, Zhengzhong Liu, Ion Stoica, Eric Xing, and Hao Zhang. Vsa: Faster video diffusion with trainable sparse attention. *arXiv preprint arXiv:2505.13389*, 2025. [1](#), [2](#), [3](#), [5](#), [7](#), [8](#)